Using systems medicine to identify a therapeutic agent with potential for repurposing in inflammatory bowel disease

DOI:
10.1242/dmm.044040

Document Version
Final published version

Published in:
DMM Disease Models and Mechanisms

First posted online on 21 September 2020 as 10.1242/dmm.044040
Access the most recent version at http://dmm.biologists.org/lookup/doi/10.1242/dmm.044040

Using systems medicine to identify a therapeutic agent with potential for repurposing in Inflammatory Bowel Disease

Authors:

Katie Lloyd[1]*, Stamatia Papoutsopoulou[1,2]*, Emily Smith[2], Philip Stegmaier[3], Francois Bergey[4], Lorna Morris[4], Madeleine Kittner[4], Hazel England[2], Dave Spiller[2], Mike HR White[2], Carrie A Duckworth[1], Barry J Campbell[1], Vladimir Poroikov[5], Vitor AP Martins dos Santos[4], Alexander Kel[3], Werner Muller[2], D Mark Pritchard[1], Chris Probert[1], Michael D Burkitt[1,2], the SysmedIBD consortium[6].

* These authors contributed equally

Affiliations:

1: Department of Cellular and Molecular Physiology, University of Liverpool, Liverpool, UK

2: Faculty of Biology Medicine and Health, University of Manchester, Manchester, UK

3: geneXplain GmbH, Wolfenbuettel, Germany

4: LifeGlimmer GmbH, Berlin, Germany

5: Institute of Biomedical Chemistry, Moscow, Russia

6: www.sysmedIBD.eu

Contact Details:

Dr Michael Burkitt
Division of Diabetes, Endocrinology
& Gastroenterology
School of Medical Sciences
Faculty of Biology, Medicine & Health
Michael Smith Building,
Dover Street,
Manchester,
M13 9PT

Email: michael.burkitt@manchester.ac.uk

Abstract:

Objective: Inflammatory bowel diseases cause significant morbidity and mortality. Aberrant NF-κB signalling is strongly associated with these conditions, and several established drugs influence the NF-κB signalling network to exert their effect. This study aimed to identify drugs which alter NF-κB signalling and may be repositioned for use in inflammatory bowel disease.

Design: The SysmedIBD consortium established a novel drug-repurposing pipeline based on a combination of in-silico drug discovery and biological assays targeted at demonstrating an impact on NF-kappaB signalling, and a murine model of IBD.

Results: The drug discovery algorithm identified several drugs already established in IBD, including corticosteroids. The highest-ranked drug was the macrolide antibiotic Clarithromycin, which has previously been reported to have anti-inflammatory effects in aseptic conditions.

Clarithromycin's effects were validated in several experiments: it influenced NF-κB mediated transcription in murine peritoneal macrophages and intestinal enteroids; it suppressed NF-κB protein shuttling in murine reporter enteroids; it suppressed NF-κB (p65) DNA binding in the small intestine of mice exposed to LPS, and it reduced the severity of dextran sulphate sodium-induced colitis in C57BL/6 mice. Clarithromycin also suppressed NF-κB (p65) nuclear translocation in human intestinal enteroids.

Conclusions: These findings demonstrate that *in-silico* drug repositioning algorithms can viably be allied to laboratory validation assays in the context of inflammatory bowel disease; and that further clinical assessment of clarithromycin in the management of inflammatory bowel disease is required.

Keywords:

Inflammatory Bowel Diseases

NF-kappa B

Drug Repositioning

Interdisciplinary research

Organoids

Macrolide

Ulcerative colitis

Crohn’s disease

Introduction:

Inflammatory bowel diseases (IBD) affect 0.5-1.0% of people in the Western world and cause substantial morbidity and cost to society(Feagan et al., 2014; van Deen et al., 2014). The aetiology of IBD is complex. There are aberrant inflammatory responses, leading to mucosal damage and the disease phenotype.

Diverse therapeutic approaches are employed: Many patients with mild ulcerative colitis are treated with mesalazine preparations, which predominantly act topically on the colonic mucosa to suppress inflammation(Marteau et al., 2005), others require systemic therapy with highly-specific biologic agents targeting inflammatory mediators(Baert et al., 1999; Targan et al., 1997). While these drugs have very different mechanisms of action, they influence host inflammatory responses and either directly or indirectly alter NF-κB signalling.

The NF-κB signalling network is a tightly-controlled, dynamically-regulated signal transduction pathway with several well-described transcription regulatory feedback loops(Lev Bar-Or et al., 2000): this orchestrates innate immune responses by regulating transcription through dimers of the five NF-κB proteins (RelA(p65), RelB, NF-κB1(p50), NF-κB2(p52) and c-Rel). Signalling through this network is characterised by the oscillation of NF-κB proteins between the cytoplasm and nucleus; most clearly demonstrated for the RelA(p65) subunit(Nelson et al., 2004). In addition to changes in the inflammatory milieu, this network also affects several other processes which are dysregulated during chronic gastrointestinal inflammation including cell turnover, DNA damage responses and cell senescence(Perkins, 2012). Several studies have associated aberrant NF-κB signalling with IBD (reviewed in (Atreya et al., 2008; McDaniel et al., 2016; Merga et al., 2016).

Because of the complexity of NF-κB signalling, targeting specific components of the network has not been a successful drug development strategy to date, mainly because of the

ubiquitous nature of NF-κB signalling. The impact of gross inhibition of critical members of the NF-κB signalling cascade has been unpredictable and associated with undesirable off-target effects. The complexity of NF-κB signalling during GI tract inflammation is elegantly demonstrated by murine work. When transgenic mice lacking specific NF-κB sub-units were subjected to a DSS model, mice lacking *cRel* and *Nfkb1* developed more severe colitis than wild-type controls, whilst *Nfkb2-/-* mice were resistant to colitis(Burkitt et al., 2015). C57BL/6 mice lacking IKKbeta in epithelial cells were more severely affected by DSS colitis(Greten et al., 2004), whilst IL-10-/- mice lacking IKKbeta in the intestinal epithelium had similar colitis to those with intact NF-κB signalling but in both these models loss of IKKbeta in myeloid cells attenuated colitis and improved survival(Eckmann et al., 2008). It is therefore likely that the transcriptomic effects of attenuating NF-κB signalling in the epithelium and myeloid compartments is different.

This complexity has promptied calls for highly specific inhibitors which target components of the network in precisely-selected cell types(Baud and Karin, 2009). This approach is useful in certain circumstances such as multiple myeloma, where targeting a specific cancer cell lineage is desirable and may be achievable. In contrast, for complex benign inflammatory diseases, including IBD, this strategy is less likely to be successful due to challenges in identifying a specific target cell population.

We propose an alternative strategy, to 'nudge' an individual's NF-κB signalling network towards an idealised healthy phenotype. This approach may offer a more pragmatic way of targeting aberrant NF-κB signalling, without the limitations of selective tissue targeting or gross pathway inhibition.

To investigate this in the context of inflammatory bowel disease, we used a combination of novel bioinformatic analyses and laboratory studies to identify agents likely to impact NF-κB

signalling and inflammatory bowel disease. Because of the divergent roles of myeloid and epithelial NF-κB signalling during GI tract inflammation, we have established assays to measure the effects of drugs on both epithelial and immune tissues. We then validated the efficacy of the most highly ranked agent, both in terms of inhibiting NF-κB activity, and modulating an *in-vivo* model of colitis.

Methods:

Motif Enrichment Analysis using Logistic Regression (MEALR)

Transcription regulatory feedback loops driven by NF-kappaB/RelA and cooperating transcription factors were inferred based on existing knowledge about signalling pathways involving NF-kappaB/RelA transcription factor binding motifs and ChIP-seq experiment data targeting NF-kappaB/RelA-bound sites in the human genome. The analyses were mainly conducted using the geneXplain platform(Koschmann et al., 2015).

Our analysis aimed to identify feedback loops that encompass components of NF-kappaB/RelA pathways as well as cooperating transcriptional regulators that are themselves regulated by NF-kappaB/RelA (Figure S1).

First, we applied a novel method for motif enrichment analysis using logistic regression (MEALR). MEALR was developed to analyse binding site combinations in sets of DNA sequences that are likely to be bound by a common set of transcriptional regulators, as obtained through ChIP-seq experiments. The algorithm chooses a small set of DNA-sequence motifs from a possibly large library of such models. Given N sequences assigned to classes $y_i \in \{0,1\}$ and a library of M positional weight matrices (PWMs), MEALR estimates a sparse logistic regression (LR) model

$$P(y|x) = \frac{1}{1+e^{-(\beta_0+\sum \beta_k x_k)}}$$

using the vector of sequence scores calculated for the ith sequence

$$x_{ik} = \log\left(\frac{1}{L_i}\sum_w \exp(S_w)\right); i = 1..N, k = 1..M$$

where S_w is the log-odds score of the PWM assigned to the wth sequence window. The model coefficients can be used to prioritize motifs of transcriptional regulators with respect to their importance for experimentally observed binding events. Combinations of motifs prioritized by MEALR tend to coincide with transcription factors that are known to cooperate.

We applied MEALR to reveal discriminative DNA-sequence motifs in genomic regions bound by NF-kappaB/RelA after TNF-alpha stimulus. Sequence scores were calculated for a subset from the TRANSFAC(R) database, release 2014.4, consisting of 1429 motifs for transcription factors from vertebrate organisms. Genomic NF-kappaB/RelA binding sites were identified by analysis of ChIP-seq experiments carried out by the ENCODE project [Encode] and deposited in GEO [Gm10847, Gm12878, Gm12891, Gm12892, Gm15510, Gm18505, Gm18526, Gm18951, Gm19099, and Gm19193 (GEO series GSE31477)]. MEALR models were estimated to distinguish ChIP-seq peak sequences from genomic background sequences that were randomly sampled from gene promoter regions not overlapping with peaks of the respective experiment. The analysis was conducted five times for each ChIP-seq data set with different background sequence sets. We retained motifs that were incorporated in the model in all five runs. As MEALR may select similar binding motifs with different identifiers in separate runs, we considered DNA-sequence motif similarity quantified by our method m2match(Stegmaier et al., 2013).

A total of 62 TRANSFAC(R) motifs were selected by MEALR in at least 9 of the 10 ChIP-seq data sets. These motifs mapped to 38 transcription factor genes including NF-κB-type factors as well as other transcription factors which our analysis suggests cooperate with NF-κB (Supplementary Table S7).

To identify potential consensus target genes of NF-kappaB/RelA we grouped overlapping peak regions and mapped groups with peaks in at least 6 out of 10 ChIP-seq experiments to nearby genes. This part of the analysis focused on peaks with a maximal length of 3000 bases (>99.1% of all peak regions in the ten ChIP-seq experiments). 4835 consensus ChIP-seq regions were identified in the vicinity of 6329 genes. These genes were defined as consensus target genes. Among the target genes we identified 24 transcription factors inferred by MEALR as well as 90 of 284 genes encoding components of signalling pathways and cascades involving NF-kappaB/RelA collected from the TRANSPATH(R) database, release 2013.3. These comprise the feedback loops with NF-kappaB/RelA consensus targets described in Figure S1.

Pathway analysis for master regulator search

Molecules that regulate the expression of differentially expressed genes through control of the activity of NF-κB sub-units were defined as master regulators and were identified by applying a key-node analysis algorithm(Kel et al., 2006), using the TRANSPATH® database of gene regulatory and signal transduction pathways(Krull et al., 2006).

Key-nodes were prioritised based on the weighted ratio between the number of molecules from the input set that could be reached from the key-node in ≤10 steps and the total number of reachable nodes. The higher the score, the greater the chance that the key-node plays a master regulatory role.

In-silico drug discovery

Relationships between the chemical structure of compounds and their biological activities were analysed using large-scale prediction of activity spectra(Filimonov et al., 1995; Poroikov et al., 2001) (http://genexplain.com/pass/) to discover potential new drugs for IBD treatment. The PASS algorithm is based on Bayesian estimates of probabilities of molecules belonging to the classes of active and inactive compounds(Filimonov et al., 2014). The predicted activity spectrum is presented in PASS by the list of activities with probabilities "to be active" Pa and "to be inactive" Pi calculated for each activity.

For each compound of the tested library, a cumulative score was computed across the 46 PASS activities selected in the previous analysis.

$$Score = \sum_{i=1}^{46} p_a(i)$$

here $p_a(i)$ is the probability for the given compound to be active for each activity *i*.

For each compound tested, the cumulative score was required to be higher than 3.0, and the Pa for the PASS activity “Transcription factor NF-κB inhibitor” was positive.

Patient recruitment and ethics

Samples used for the generation of human enteroids were donated by patients without evidence of IBD attending for colonoscopy at the Royal Liverpool and Broadgreen University Hospitals NHS Trust. Samples were collected following written informed consent and favourable ethical opinion from North West-Liverpool East Research Ethics Committee (15/NW/0045).

Animal maintenance and welfare

All animal breeding, maintenance and procedures were performed under a UK Home Office licence, with local Animal Welfare and Ethics Review Board approval. Transgenic animals were

maintained at the University of Manchester. Wild-type mice were purchased from Charles River (Margate, UK) and maintained either at the University of Manchester or University of Liverpool in SPF facilities with access to standard chow and drinking water *ad-libitum* unless otherwise specified. Standard 12-hour light/dark cycles were used; standard temperature and humidity levels were maintained.

Transgenic mouse strains

Human TNFα luciferase mice (hTNF.LucBAC)

This line has been engineered to have a bacterial artificial chromosome (BAC) expressing luciferase under the regulation of the entire human TNF promoter. Primary cultures established from this mouse enable direct measurement of TNF promoter activity in a non-transformed *ex-vivo* system(Minshawi et al., 2019).

Human p65-DsRedxp/IκBalpha-eGFP mouse (p65-DsRedxp/IκBalpha-eGFP).

This line expresses fusion proteins of NF-κB(p65) and the *Discosoma* red fluorescent protein – Express (DsRedxp) under the regulation of the native human p65 promoter, and IκBalpha and enhanced green fluorescent protein (eGFP), regulated by the human IκBalpha promoter(Dudek et al., 2017). Primary cultures established from this mouse enable direct visualisation of these fusion proteins.

Peritoneal macrophage isolation, in vitro culture and luciferase assay

Resident peritoneal macrophages were obtained from mice by standard methods. Cells were stimulated with either 10ng/mL LPS (*Salmonella enterica* serovar Minnesota R595; Calbiochem), TNF (R&D Systems) at 40 ng/mL, muramyl dipeptide (MDP, Invivogen) at 10µg/mL or Flagellin (Novus Bio) at 500ng/ml. Luciferase activity was measured over time in a CO_2 luminometer (Lumistar Omega, BMG Labtech).

Flow Cytometry

Peritoneal macrophages were stimulated with 1µg/ml LPS for 20min. Fixed cells were stained for phosphor-p65 (pre-diluted PE Mouse anti-NF-κB p65 (pS529), BD Bioscience, clone K10-895.12.50) and analysed by flow cytometry using an LSRII Cytometer (BD). Data analyses were performed with FlowJo887 software (Tree Star).

Primary Epithelial cell culture

Enteroids were generated from human and murine tissue using modifications of established protocols. Tissue samples were disaggregated by calcium chelation in EDTA followed by mechanical disaggregation in a sucrose/sorbitol solution. Crypt pellets were resuspended in Matrigel (Corning, UK) and were maintained in media containing a combination of recombinant growth factors and growth factor containing conditioned media (supplemental methods). Enteroids were passaged at least once prior to experiments.

Wnt-3a conditioned media

L Wnt-3a cells (ATCC® CRL-2647™) were seeded into a T75 flask and passaged when ~80% confluent into another T75 flask with 10mL selection media of Dulbecco's modified eagle's medium (DMEM) supplemented with 10% foetal calf serum (FCS), 2mM penicillin-streptomycin and 300µg/ml zeocin (Invivogen). When confluent, cells were passaged at a 1:4 split ratio into T150 flasks and 15ml selection media was added. After 24hrs, cells were washed with PBS and the media was changed to 10 mL reduced serum media of DMEM supplemented with 5% FCS and 2 mM penicillin-streptomycin and grown until over-confluent (approximately 4-5 days). The media was collected and centrifuged at 2000 x *g* for 5mins at 4°C. The supernatant was filtered through a 0.22 µm syringe filter (Millipore) and stored at -80°C until use.

Basal murine organoid media

This media consisted of Advanced DMEM/F12 media (Sigma) supplemented with 2mM Glutamax-I (ThermoFisher), 10mM Hepes (Sigma), 1x N2 and B27 growth factors (both Invitrogen and 1x antibiotic/antimycotic mixture (Thermofisher).

Human seeding media

Seeding media contained 50% human basal media and 50% Wnt-3a conditioned media with the addition of 50ng/mL hEGF, 100ng/mL hNoggin, 1µg/mL hR-Spondin-1 (all R&D systems), 1mM N-acetylcysteine (Sigma), 10mM Nicotinamide (Sigma), 10nM Gastrin (Bachem), SB202190 10µM, 0.01µM PGE2, 0.5µM LY2157299.

Human organoid culturing media

Seeding media contained 50% human basal media and 50% Wnt-3a conditioned media with the addition of 50ng/mL hEGF, 100ng/mL hNoggin, 0.5µg/mL hR-Spondin-1 (all R&D systems), 10mM Nicotinamide (Sigma), 10nM Gastrin (Bachem), SB202190 10µM, 0.01µM PGE2.

Human organoid culture

Five ileal biopsies were taken from non-IBD patients that were enrolled onto the SysMedIBD study and placed into 1 ml PBS containing 1x antibiotic-antimycotic (PBSAA) for transport to the laboratory. In a fume hood, biopsies were washed 10 times in 2 mL PBSAA. Biopsies were places in 4 mL ice cold chelation buffer (3 mM EDTA in PBS) and incubated at room temperature for 30 mins without agitation. Chelation buffer was discarded and replaced with 4 mL shaking buffer (43.3 mM sucrose and 59.4 mM sorbitol in PBS). Biopsies were mechanically agitated in the shaking buffer for 3 mins or until the crypts were no longer seen

on the biopsy surface. The crypt suspension was pelleted by centrifugation at 200g for 5mins at 4°C, resuspended in 500 µL Matrigel (Corning, UK) and 50µL was plated out per well of a 24 well plate. Matrigel was polymerised at 37°C before applying 500 µL of human seeding medium per well. After 3 days, human seeding medium was changed to fresh human culturing media which was replaced every 3 days. Organoids were passaged every 7 days.

Terminal ileal organoids were passaged and cultured for 5 days before being removed from the Matrigel using 400 µL cell recovery solution (Corning) on ice for 40 mins. The organoid suspension was transferred to a 15 mL Falcon tube and centrifuged 200 x *g* for 5 mins. The organoids were washed in PBS and resuspended in fresh human culturing media. Pre-treatment with or without 10 µM clarithromycin or 1% DMSO (vehicle control) was applied in suspension for 30 mins. Following pre-treatment, 100 ng/mL recombinant human TNF (Peprotech) was applied for a further 30 mins and then fixed with 4% paraformaldehyde for 20 mins. Fixed organoids were washed with PBS twice and transferred into 300 µL Richard-Allan™ Histogel™ (Thermofisher) and left to polymerise on ice for 30 mins. Once set, the organoid-containing Histogel sample was processed as normal and paraffin embedded.

Enteroid immunohistochemistry

Enteroids were pre-treated with 10µM clarithromycin or 1% v/v DMSO (vehicle) for 30mins. Following pre-treatment, 100ng/mL recombinant human TNF (Peprotech) was applied for a further 30mins. Fixed enteroids were transferred into Richard-Allan™ Histogel™ (Thermofisher) and processed for histology. Immunohistochemical analysis was performed to visualise p65 (Cell Signaling Technologies, #8242, 1:100).

Enteroids were selected for scoring based on size criteria, enteroids with fewer than 20 cells per circumference were excluded from analysis, the average number of cells scored per enteroids was 118 (range 46-239). The proportion of cells nuclear stained for p65 was

quantified for each organoid using manual cell counting by a scorer experienced in quantitative histological techniques (KL) and blinded to experimental conditions for each sample. First, for one circumferance of an organoid, all nuclei were counted using a handheld tally counter. Immediately afterwards, the same section was scored for number of positively stained nuclei and the percentage of positively stained nuclei per organoid circumference calculated. For each patient at least 4 enteroids were assessed, and there were 6 patients represented per group. Statistical testing was based on N=6 patients.

Murine intestinal organoid confocal microscopy

Proximal enteroids from p65-DsRedxp/IκBalpha-eGFP dual-reporter mice were passaged into glass-bottom dishes (Thermo Scientific™ Nunc™ Glass Bottom Dishes) in phenol red-free complete media. Images were taken for 6-8 enteroids per dish using a Zeiss Laser Scanning Microscope (LSM880) with a C-Apochromat 40x/1.2 W Korr FCS M27 objective. Enteroids were imaged for 30mins before treatment with 10µM clarithromycin or 1% v/v DMSO vehicle. Thirty minutes later, cultures were stimulated with 100ng/ml TNF and imaged for a further 3hrs. Images and videos were processed using Zen 2011 software and CellTracker (Warwick Systems Biology Centre).

LPS-induced NF-κB activation in mice

Groups of adult (8-10-week-old) male C57BL/6 mice received 50mg/kg clarithromycin i.p, or vehicle daily for three days. Following a 3-day washout period, either 50mg/kg clarithromycin i.p., or 0.9% w/v saline vehicle was administered, the next day either 50mg/kg clarithromycin i.p. or vehicle was followed by either 0.125mg/kg ultrapure LPS from *E. coli* K12 (Invivogen) i.p. or 0.9% w/v saline vehicle. Animals were culled 90 minutes after LPS/vehicle administration; small intestinal mucosal scrapes were prepared in RIPA buffer with protease

inhibitors (Sigma, Gillingham, UK). NF-κB p65 DNA binding was quantified using a TransAM DNA-binding ELISA (ActiveMotif, La Hulpe, Belgium).

Dextran sulphate sodium-induced colitis

Groups of adult (8-10-week-old) male C57BL/6 mice were administered either 10 mg/kg clarithromycin, or vehicle by orogastric gavage daily for four days. Following a washout period, animals received 2.5% DSS in drinking water, for five days. Animals recovered for a further three days. From the start of DSS treatment to termination of the experiment either 10 mg/kg clarithromycin or normal saline vehicle was administered by daily orogastric gavage. Tissue samples were harvested and prepared for histological analysis, including quantitative histology, as previously described(Williams et al., 2016).

Statistical analysis of laboratory work

Statistical analyses were performed using GraphPad Prism v.7.0 software. Specific statistical tests are annotated in the text and figure legends. Reported *p*-values are two-tailed. Normality testing was performed with the D'Agostino & Pearson test.

Results:

To predict drugs that may influence disrupted NF-κB signalling in IBD, a drug-discovery strategy combining data from multiple sources (archived ChIP-seq analyses; natural language text-mining of published abstracts; data from IBD GWAS analyses; and known IBD biomarkers and drug targets curated in the HumanPSD database) was developed (Figure 1).

Developing an enhanced NF-κB signalling network

Signalling molecules comprising (transcription) regulatory feedback loops present promising drug targets because they can influence the dynamics of a signalling pathway of interest, including the TNF-alpha/NF-κB pathway. To augment existing knowledge about NF-κB

signalling, we developed an analysis workflow to identify genes encoding potential components of transcription regulatory feedback loops combining known NF-κB-involving signalling pathways, ChIP-seq assay based NF-κB/RelA-bound genomic regions from the ENCODE project (GEO series GSE31477), and a newly-developed method to find combinations of enriched DNA-sequence motifs (Motif Enrichment Analysis by Logistic Regression (MEALR)) (see supplementary materials for details). Combinations of prioritised motifs tend to coincide with transcription factors that are known to cooperate. Our analysis found 24 transcription factors that appear to cooperate in NF-κB signalling within the genomic regions reported by ENCODE (Table 1) as well as 90 potential NF-κB/RelA-target genes that encode components of known pathways. (Table 2). The results were used to annotate the TRANSPATH® database of mammalian signal transduction and metabolic pathways.

Text mining to establish context proteins and genes for up-stream network analyses

1000 relevant abstracts were retrieved using the MedlineRanker tool(Gijon-Correas et al., 2014) from the PubMed database using the MeSH terms “Inflammatory bowel diseases” and “NF-κB”. Protein-protein interactions were identified in these abstracts using PESCADOR(Barbosa-Silva et al., 2011). PESCADOR detects genes, proteins and their interactions, and rates them based on co-occurrences in an abstract. 827 interactions common for both *Homo sapien*s and *Mus musculus*, 2 for *Mus musculus* alone, and 26 uniquely for *Homo sapiens* were extracted (Supplementary Table S1). After querying the TRANSPATH® database for known direct interactions, 127 novel co-occurrences of genes or proteins in the abstracts analysed. This table of interactions was used to provide context to subsequent up-stream network analysis to impute the key regulatory nodes for NF-κB signalling in IBD.

Identifying master regulators of the NF-κB signalling network

An upstream search of the various molecular components of NF-κB complex including: NF-κB1-isoform1, NF-κB1-isoform2, NF-κB2-isoform4, NF-κB2-p100, NF-κB2-p49, RelA-p35, RelA-p65-delta, RelA-p65-delta2, RelA-p65-isoform1, RelA-p65-isoform4, RelB, c-Rel was performed. The network search extended to a maximal radius of 10 steps upstream of the NF-κB components and used a false discovery rate (FDR) cut-off of 0.05 and Z-score (reflecting how specific each master regulator was) cut-off of 1.0. The list of interacting proteins obtained by text-mining was used to provide "Context proteins" for the master-regulator acquisition algorithm(Kel et al., 2016). This analysis revealed 325 controlling nodes predicted to exert signalling activity for the NF-κB components (Table S2).

Developing a list of IBD associated genes and potential therapeutic targets

A list of IBD associated-genes and potential therapeutic targets was established by retrieving information from the HumanPSD database including known IBD biomarkers and drug targets, and two lists of IBD-related genes from genome-wide association studies, one focused on revealing genes of IBD prognosis(Lee et al., 2017), and another on IBD susceptibility(Hasler et al., 2017). 159 IBD-targets were identified and summarised with an indication of the source of evidence about their relevance to IBD (Table S3).

Finally, to produce a list of proposed therapeutic targets the list of IBD-targets was intersected with the 325 controlling nodes to obtain 62 candidates (defined as IBD key-nodes, Table S4) that represent genes predicted to influence IBD associated NF-κB regulation, which had also independently been identified as IBD associated genes or potential therapeutic targets.

Predicting drugs that may influence the IBD key-nodes

The PASS software package was used to predict drugs which may interact with IBD key-nodes: this software predicts the ability of a chemical structure to interact and influence the activity of defined molecular targets and biological activities.

The 62 key-nodes were translated into 46 PASS activities (Table S5). To identify compounds with potential for clinical re-positioning, the Top 200 drugs library was analysed to predict the probability that these established, and licenced agents may interfere with each PASS activity. A cumulative score was calculated across all 46 PASS activities for each drug. We also required that the drugs were predicted to be active against the PASS activity "Transcription factor NF κB inhibitor".

29 compounds achieved these criteria (Table 3); importantly, this table included several corticosteroids already used to treat IBD, supporting the validity of the discovery strategy.

The highest-ranked drug was a macrolide antibiotic: clarithromycin. This agent is of particular interest because macrolides have an established role in treating aseptic inflammatory conditions including chronic rhinosinusitis(Oakley et al., 2017) and panbronchiolitis(Lin et al., 2015) and because clarithromycin has previously been trialled in IBD with divergent outcomes(Leiper et al., 2008; Leiper et al., 2000). We, therefore, considered it to be an excellent candidate for strategic repurposing and have used clarithromycin as a paradigm molecule for the development of a mechanism-led drug validation pathway.

Clarithromycin suppresses stimulus-induced luciferase activity in primary cell cultures.

To validate the efficacy of clarithromycin as an inhibitor of NF-κB mediated transcription, primary cultures from the hTNF.LucBAC mouse, a transgenic line that expresses firefly luciferase under the control of the entire human *TNF* promoter(Minshawi et al., 2019), were used.

Luciferase activity was triggered by ligand binding to the TNF receptor and pattern recognition receptors including TLR4 (lipopolysaccharide), TLR5 (flagellin) and NOD2 (muramyl dipeptide, MDP) (Figures 2A-D) in peritoneal macrophages harvested from this mouse. When cells were pre-treated for 30 minutes with 10μM or 100μM clarithromycin, a dose-dependent reduction in luciferase activity was observed, independent of the stimulus applied.

The effect of clarithromycin on NF-κB activation in murine peritoneal macrophages was confirmed by isolating peritoneal macrophages from 4 WT mice, and treating them with 10μM clarithromycin or vehicle before stimulation with 1μg/ml LPS. Cells were fixed, stained for phosphorylated-p65 and quantified by flow cytometry. Median fluorescence intensity (MFI) increased on stimulation (p=0.03, ANOVA); co-administration of LPS and clarithromycin suppressed this response (p=0.008, Figure 2E).

Small intestinal organoids (enteroids) were established from hTNF.LucBAC mice to determine whether clarithromycin could also alter NF-κB responses in gastrointestinal epithelial cell cultures. Luciferase activity was detectable in these cultures in response to 100ng/mL TNF administration (Figure 3A and B). Luciferase activity was significantly suppressed by pre-treatment for 30 minutes with either 1μM (p=0.014) or 10μM (p=0.001) clarithromycin (Figure 3B and C).

Clarithromycin suppresses TNF-induced NF-κB(p65) shuttling in enteroids

To assess whether clarithromycin influenced NF-κB protein shuttling dynamics, enteroid cultures from reporter mice expressing p65-DsRedxp/IκBalpha-eGFP were established. This mouse expresses human p65-DsRedxp and human IκBalpha-eGFP fusion proteins. We used these organoids in live-cell confocal imaging studies to observe the nuclear translocation of p65 in real-time. Images were analysed using CellTracker software(Ashall et al., 2009), which allows painstaking quantification of nuclear shuttling of fluorescently labelled proteins.

Administration of 100ng/mL TNF-induced synchronised p65 translocation to the nucleus of cells within enteroids with a periodicity of approximately 50 minutes. This was observed as a highly damped shuttling response, with a single wave of synchronised nuclear translocation, followed by a second wave of partially synchronised translocation, after which further nuclear localisation occurred in an apparently stochastic fashion (Figure 4A and B and supplementary video). When cultures were pre-treated with 10µM clarithromycin for 30 minutes, p65-DsRedxp nuclear translocation was markedly suppressed.

To quantify these events more precisely the mean area under the curve (AUC) during the first oscillatory wave (Figure 4D) was calculated, and demonstrated decreased nuclear intensity of p65-DsRed fluorescence in clarithromycin pre-treated enteroids (p=0.005). The time to peak nuclear fluorescence after 100ng/mL TNF administration was also quantified (figure 4E). In DMSO vehicle-treated cells, peak fluorescence occurred at a median time of 47.2 (IQR 41.0-47.2) minutes. This was not significantly different for clarithromycin treated enteroids, but there was significantly more distance from median time of peak fluorescence observed in clarithromycin treated than vehicle-treated cells (p<0.0001, figure 4F). To assess synchronisation of nuclear translocation, the time between peak fluorescence and median time for peak nuclear fluorescence was calculated for each cell (Figure 4F). This confirmed an 8-fold greater variation in timing for peak nuclear fluorescence in CLA treated enteroids compared to controls (p<0.0001), confirming that the synchronisation of p65 nuclear translocation was lost following exposure to CLA.

Clarithromycin suppresses LPS-induced NF-κB (p65) DNA binding in-vivo

To determine whether the effects of clarithromycin on stimulus-induced NF-κB activity observed *in-vitro* also occurred *in-vivo*, 0.125mg/kg LPS was administered to groups of six C57BL/6 male mice by intraperitoneal injection, either with or without clarithromycin co-

administration. This stimulus induces small intestinal epithelial cell shedding, regulated by both NF-κB1 and NF-κB2 signalling pathways(Williams et al., 2013).

LPS administration induced a 2-fold increase in p65 DNA binding, compared to saline vehicle control (p<0.001, 1-way ANOVA and Dunnett's posthoc test); pre-treatment with clarithromycin suppressed this effect by approximately 51% (p=0.007, Figure 5A).

Clarithromycin suppresses DSS-induced colitis

To determine whether clarithromycin affected murine colitis *in-vivo, c*larithromycin or vehicle were administered to mice receiving DSS to induce colitis. Animals received clarithromycin or vehicle daily for four days by oro-gastric gavage, after a four-day washout period 2.5% w/v DSS in drinking water *ad-libitum* was commenced for five days, followed by recovery for a further three days.

Mice co-administered DSS and clarithromycin lost significantly less weight than other groups (p=0.039, 1-way ANOVA and Dunnett's posthoc test, Figures 5B and 5C) and had lower compound histology scores (p=0.004, Figures 5D and 5F) and a higher number of surviving colonic crypts than mice treated with vehicle (p=0.017, Figure 5E); this suggests that clarithromycin at least partially ameliorates this model of colitis.

Clarithromycin suppresses TNF-induced NF-κB (p65) nuclear localisation in human enteroids

To determine whether the effects identified in murine primary culture and *in-vivo* experiments were also relevant to humans, passaged human ileal organoids from individuals with no evidence of IBD were pre-treated with 10μM clarithromycin or DMSO vehicle for 30 min before stimulation with 100ng/ml TNF. Paraformaldehyde fixed cultures were immunostained for p65, and the percentage of cells expressing nuclear-localised p65 was quantified. In untreated human enteroids, 0.6% (SEM 0.37) of cells demonstrated p65 nuclear localisation, administration of TNF induced a 57-fold increase in cells expressing nuclear p65

(33%, +/- 3.2 SEM, $p<0.0001$, 1-way ANOVA and Dunnett's posthoc test, N=6 per group). Pre-treatment with clarithromycin suppressed TNF-induced nuclear localisation of p65 to a level comparable with DMSO vehicle-treated enteroids. (1%, +/- 0.36 SEM, $p<0.0001$, Figure 6).

Discussion:

This article demonstrates that the macrolide antibiotic clarithromycin is a modifier of NF-κB signalling in the gastrointestinal tract. Identification of clarithromycin, using an *in-silico* screen of licensed drugs, demonstrates how novel bioinformatics can be used to progress drug-repurposing, a strategy that has the potential to reduce the cost of future drug development. The SysmedIBD consortium integrated diverse skill sets to develop this approach which could be applied in different ways in the future. An identical bioinformatic analysis could be used to screen panels of small molecules to identify novel therapeutics for IBD. Similarly, the system could be adapted for use in other contexts where NF-κB signalling is of paramount importance or refocussed onto different signalling networks.

Our list of drugs predicted to influence IBD outcomes included several drugs in routine use for IBD, most prominently the corticosteroids, which are used to treat acute relapses of inflammatory bowel disease(Truelove and Witts, 1955; Turner et al., 2007). The analysis also identified sex hormones including medroxyprogesterone and estradiol which have been shown to modulate colitis(Armstrong et al., 2017), and colitis-associated adenoma development *in vivo*(Son et al., 2019); and non-steroidal anti-inflammatory drugs, which, in clinical practice, are identified as agents that exacerbate IBD(Long et al., 2016). The harmful effects of NSAIDs result from inhibition of constitutively expressed COX-1 in the gastrointestinal epithelium, causing epithelial damage and ulceration; inhibition of COX-2, which is upregulated at sites of inflammation is a well-established anti-inflammatory mechanism, which influences NF-κB signalling. The drug discovery approach deliberately

included a bias for agents that alter NF-κB signalling; it is likely that NSAIDs have been selected because of this bias.

These observations demonstrate the importance of interdisciplinary working. The *in-silico* drug discovery model is a powerful tool to identify drugs that may be repurposed, but decisions about which agents to pursue for further analysis can only be made in the context of existing clinical literature.

Laboratory evaluation of clarithromycin aimed to demonstrate proof-of-principle that a drug identified by *in-silico* testing would demonstrate the predicted mechanism of action, and show efficacy *in-vivo*.

Our strategy has potential for development into a higher throughput compound screening system: for example, the hTNF.LucBAC macrophage assay can be performed in a 96-well plate format, and peritoneal macrophages are abundant, simple to extract and highly sensitive to stimulus. Reporter enteroids generated from hTNF.LucBAC mice allowed us to validate the findings seen in peritoneal macrophages in a relevant, untransformed epithelial model using comparable technology, but are unlikely to be amenable to high-throughput assay development due to the challenges (and cost) of maintaining a 3D culture in a small well in a culture plate.

The visualisation of p65.DsRed translocation between the nucleus and cytoplasm in enteric organoids is technically challenging, and not immediately scalable. One of the challenges that we persistently encountered was fluctuating fluorescence prior to stimulation with TNF, despite efforts to rest the cells prior to imaging. Unlike a monoculture of immune cells enteroids are a complex system with several cell types represented within the organoid structure. Whether this is due to paracrine secretion between different cells within the organoid structure, or is a factor related to organoid culture conditions is not possible to

dissect currently. Our assays also demonstrated fundamental differences in NF-κB signalling dynamics compared to cancer cell lines(Harper et al., 2018; Nelson et al., 2004), with TNF-induced p65 oscillations being heavily damped in organoids. This observation demonstrates the value of untransformed primary culture; the mechanisms underlying these differences will be subject to further investigation.

The observation that intestinal NF-κB signalling is altered by clarithromycin *in-vivo* is in keeping with earlier work using cancer cell lines(Peng et al., 2014), but it is the first demonstration that macrolides alter this signalling pathway in either untransformed enteroids or gastrointestinal mucosae *in vivo*.

Previous studies demonstrated that a non-antibiotic macrolide, CSY0073, influenced acute DSS colitis in C57BL/6 mice(Mencarelli et al., 2011), but clarithromycin had not been studied. Our murine experiments were complicated by the antibiotic effects of Clarithromycin. Murine models of colitis are known to vary dependent on animal house conditions and host enteric microbiota. Several strategies could have been adopted to help differentiate antibiotic and anti-inflammatory effects of clarithromycin, all of which are flawed. Germ free mice and gnotobiotic mice have been used to impute impacts of gut microbiota in inflammatory bowel disease models, but they are flawed as immune systems development is divergent in germ free mice. Broad spectrum antibiotics have been usedin an attempt to eradicate commensal enteric bacteris, but no antibiotic combination will effectively achieve this goal, and its effect on the mycobiome and virome would be unquantifiable.

We preferred to adopt a consistent approach that was based on pre-exposure to the clarithromycin. The intention of this approach was to build evidence for the antibiotic effect of CLA by examining the impact of pre-treatment with CLA, and comparing to the anti-inflammatory effects of sustained CLA treatment. In the LPS administration experiment the

timepoinrts are extremely short, therefore an antibiotic effect within the experimental period is highly unlikely to explain differences between CLA pretreated animals and animals administered CLA immediately before LPS. The antibiotic effect is a greater concern in the DSS experiment, but the inclusion of data from relevant control animals has allowed us to unpick the anti-inflammatory effect. Intriguingly the histological damage in mice pretreated with CLA was worse than that seen in the vehicle control mice, suggesting that the antibiotic effect in this model may, if anything, have the opposite effect to sustained CLA treatment.

The *in-vivo* studies rely on studying the whole organism and it was not feasible to separate epithelial and immune compartments during this study, this was one of the prime motivations for studying immune and epithelial models *in-vitro*

Our final validation was to characterise whether clarithromycin influenced human epithelial NF-κB signalling. We investigated this using a HeLa reporter cell-line model, which is fast, inexpensive, commercially available and could be adapted as a high throughput screening test (figure S2), but it is inferior to the hTNF.LucBAC mouse primary culture models as NF-κB signalling is dysregulated in many cancer cell lines. By generating human enteroids, clarithromycin's effect on a primary, untransformed human epithelial cell culture could be assessed. Unfortunately, the assay used for NF-κB activation in this model was necessarily less specific, but the results supported those obtained with other assays.

It was serendipitous that the highest-ranked agent identified for repurposing was a drug that had already been trialled in IBD. Importantly the outcomes of previous trials of clarithromycin in IBD have been heterogeneous(Goodgame et al., 2001; Graham et al., 1995; Leiper et al., 2008; Leiper et al., 2000; Selby et al., 2007), suggesting that there may be context-dependent factors that determine whether clarithromycin is useful in a group of patients.

Four published papers, and a conference abstract(Graham et al., 1995) have reported the effect of clarithromycin in IBD: they all focussed on Crohn's disease and were predicated on an antibiotic effect of clarithromycin, either targeting intra-macrophage killing of *E. coli*(Leiper et al., 2008; Leiper et al., 2000) or attempting to eradicate *Mycobacterium avium paratuberculosis*(Goodgame et al., 2001; Graham et al., 1995; Selby et al., 2007).

Several factors may explain the discordant outcomes:

In all studies of clarithromycin's effect on IBD, patient inclusion was based on clinical definitions of active IBD and response assessed by clinical outcome measures. These measures lack objectivity and would not be acceptable endpoints or selection criteria for a current study.

Selby and Goodgame assessed the long-term effect of bacterial eradication; any anti-inflammatory effect would have been lost during the prolonged follow-up period before the primary endpoint was assessed.

Leiper *et al* examined an earlier timepoint when anti-inflammatory effects, could have been observed, but were not the focus of the study. Two separate cohorts of patients with clinically active Crohn's disease were recruited from a single centre; in the first study clarithromycin appeared to improve patient outcomes, but the same was not observed during the second study.

At the time, the divergent outcomes were explained by the small size of the initial study, and the relatively soft criteria for inclusion of patients with active inflammatory bowel disease. These explanations may still be valid, but an alternative hypothesis is that a sub-group of patients with active disease may respond to clarithromycin. One of the motivations for investigating existing drugs during this study was specifically to identify agents that have equivocal evidence based on traditional trials but that have evidence for an untested mechanism of action.

The current study confirms that in addition to its antibiotic effect, clarithromycin has anti-inflammatory properties, which are relevant to gastrointestinal epithelia. Further carefully designed clinical studies will be needed to test the anti-inflammatory effects of treatment with clarithromycin.

Earlier discordant trial results raise questions about trial design and patient selection. In the current era of precision medicine, it is important that patients are carefully selected for treatments, and that agents with previous dichotomous clinical trial results are revisited. To effectively review drugs for precision use, their mechanisms of action need to be understood. This study has helped us to understand how clarithromycin affects NF-κB signalling dynamics, and we hypothesise that it should be possible to select a group of clarithromycin-responsive patients based on their NF-κB signalling status.

Our consortium has recently shown that patients with IBD cluster into several different cohorts based on a dynamic measure of NF-κB responses in peripheral blood monocyte derived macrophages(Papoutsopoulou et al., 2019). We hypothesise that, by using this new measure of NF-κB activity, it will be possible to identify IBD patients most likely to respond to NF-κB targeted therapy in the form of clarithromycin, and thereby leverage a precision medicine trial.

In conclusion, our findings strongly suggest that clarithromycin may be a viable, anti-inflammatory therapeutic agent for IBD. In order to progress to a personalised medicine trial of clarithromycin in IBD a partner diagnostic test which can demonstrate altered NF-κB dynamics in patients' peripheral blood monocyte-derived macrophages is under development(Papoutsopoulou et al., 2019), once established this will be used to inform a personalised drug repurposing trial for clarithromycin in IBD.

Conflicts of Interest:

VDS is a shareholder and director of GeneXplain GmbH

AK is a shareholder and director of LifeGlimmer GmbH

Author Contributions:

KL performed experiments, acquired original data, analysed data and drafted part of the manuscript. SP performed experiments, acquired original data, analysed data and drafted part of the manuscript. ES performed experiments and acquired original data. PS developed analytical tools, analysed data and drafted part of the manuscript. FB analysed data and drafted part of the manuscript. LM analysed data and drafted part of the manuscript. MK developed analytical pathways and analysed data. HE performed experiments, acquired original data and analysed data. DS supported imaging experiments and reviewed the manuscript. MW devised the project and contributed to funding applications. CD supported organoid work and reviewed the manuscript. BC contributed to funding applications and reviewed the manuscript. VP developed analytical tools and analysed data. VMdS contributed to funding applications and supported the development of analytical pathways. AK contributed to funding applications, supported the development of novel analytical tools, performed data analyses and contributed to the drafting of the manuscript. WM contributed to funding applications and study design, reviewed the manuscript and supported laboratory work. DMP reviewed the manuscript and supported laboratory work. CP contributed to funding applications, designed the study, reviewed the manuscript and supported laboratory work. MB designed the research study, conducted experiments, analysed data, drafted the manuscript and coordinated the project.

Acknowledgements: This work was supported by the European Union Seventh Framework Programme [FP7/2012–2017] under the SysmedIBD grant, agreement no. 305564

References

Armstrong, C. M., Allred, K. F., Weeks, B. R., Chapkin, R. S. and Allred, C. D. (2017). Estradiol Has Differential Effects on Acute Colonic Inflammation in the Presence and Absence of Estrogen Receptor beta Expression. *Dig Dis Sci* **62**, 1977-1984.

Ashall, L., Horton, C. A., Nelson, D. E., Paszek, P., Harper, C. V., Sillitoe, K., Ryan, S., Spiller, D. G., Unitt, J. F., Broomhead, D. S. et al. (2009). Pulsatile Stimulation Determines Timing and Specificity of NF-κB-Dependent Transcription. *Science* **324**, 242-246.

Atreya, I., Atreya, R. and Neurath, M. F. (2008). NF-kappaB in inflammatory bowel disease. *J Intern Med* **263**, 591-6.

Baert, F. J., D'Haens, G. R., Peeters, M., Hiele, M. I., Schaible, T. F., Shealy, D., Geboes, K. and Rutgeerts, P. J. (1999). Tumor necrosis factor alpha antibody (infliximab) therapy profoundly down-regulates the inflammation in Crohn's ileocolitis. *Gastroenterology* **116**, 22-8.

Barbosa-Silva, A., Fontaine, J. F., Donnard, E. R., Stussi, F., Ortega, J. M. and Andrade-Navarro, M. A. (2011). PESCADOR, a web-based tool to assist text-mining of biointeractions extracted from PubMed queries. *BMC Bioinformatics* **12**, 435.

Baud, V. and Karin, M. (2009). Is NF-kappaB a good target for cancer therapy? Hopes and pitfalls. *Nat Rev Drug Discov* **8**, 33-40.

Burkitt, M. D., Hanedi, A. F., Duckworth, C. A., Williams, J. M., Tang, J. M., O'Reilly, L. A., Putoczki, T. L., Gerondakis, S., Dimaline, R., Caamano, J. H. et al. (2015). NF-kappaB1, NF-kappaB2 and c-Rel differentially regulate susceptibility to colitis-associated adenoma development in C57BL/6 mice. *J Pathol* **236**, 326-36.

Dudek, M., Yang, N., Ruckshanthi, J. P., Williams, J., Borysiewicz, E., Wang, P., Adamson, A., Li, J., Bateman, J. F., White, M. R. et al. (2017). The intervertebral disc contains intrinsic circadian clocks that are regulated by age and cytokines and linked to degeneration. *Ann Rheum Dis* **76**, 576-584.

Eckmann, L., Nebelsiek, T., Fingerle, A. A., Dann, S. M., Mages, J., Lang, R., Robine, S., Kagnoff, M. F., Schmid, R. M., Karin, M. et al. (2008). Opposing functions of IKKbeta during acute and chronic intestinal inflammation. *Proc Natl Acad Sci U S A* **105**, 15058-63.

Feagan, B. G., Kozma, C. M., Slaton, T. L., Olson, W. H. and Wan, G. J. (2014). Healthcare costs for Crohn's disease patients treated with infliximab: a propensity weighted comparison of the effects of treatment adherence. *J Med Econ* **17**, 872-80.

Filimonov, D. A., Lagunin, A. A., Gloriozova, T. A., Rudik, A. V., Druzhilovskii, D. S., Pogodin, P. V. and Poroikov, V. V. (2014). Prediction of the Biological Activity Spectra of Organic Compounds Using the Pass Online Web Resource. *Chemistry of Heterocyclic Compounds* **50**, 444-457.

Filimonov, D. A., Poroikov, V. V., Karaicheva, E. I., Kazarian, R. K., Budunova, A. P., Mikhailovskii, E. M., Rudnitskikh, A. V., Goncharenko, L. V. and Burov Iu, V. (1995). [The computerized prediction of the spectrum of biological activity of chemical compounds by

their structural formula: the PASS system. Prediction of Activity Spectra for Substance]. *Eksp Klin Farmakol* **58**, 56-62.

Gijon-Correas, J. A., Andrade-Navarro, M. A. and Fontaine, J. F. (2014). Alkemio: association of chemicals with biomedical topics by text and data mining. *Nucleic Acids Res* **42**, W422-9.

Goodgame, R. W., Kimball, K., Akram, S., Ike, E., Ou, C. N., Sutton, F. and Graham, D. (2001). Randomized controlled trial of clarithromycin and ethambutol in the treatment of Crohn's disease. *Aliment Pharmacol Ther* **15**, 1861-6.

Graham, D. Y., Al-Assi, M. T. and Robinson, M. (1995). Prolonged remission in Crohn's disease following therapy for *Mycobacterium paratuberculosis* infection. *Gastroenterology* **108**, A826.

Greten, F. R., Eckmann, L., Greten, T. F., Park, J. M., Li, Z. W., Egan, L. J., Kagnoff, M. F. and Karin, M. (2004). IKKβ links inflammation and tumorigenesis in a mouse model of colitis-associated cancer. *Cell* **118**, 285-296.

Harper, C. V., Woodcock, D. J., Lam, C., Garcia-Albornoz, M., Adamson, A., Ashall, L., Rowe, W., Downton, P., Schmidt, L., West, S. et al. (2018). Temperature regulates NF-kappaB dynamics and function through timing of A20 transcription. *Proc Natl Acad Sci U S A* **115**, E5243-E5249.

Hasler, R., Sheibani-Tezerji, R., Sinha, A., Barann, M., Rehman, A., Esser, D., Aden, K., Knecht, C., Brandt, B., Nikolaus, S. et al. (2017). Uncoupling of mucosal gene regulation, mRNA splicing and adherent microbiota signatures in inflammatory bowel disease. *Gut* **66**, 2087-2097.

Kel, A., Voss, N., Jauregui, R., Kel-Margoulis, O. and Wingender, E. (2006). Beyond microarrays: find key transcription factors controlling signal transduction pathways. *BMC Bioinformatics* **7 Suppl 2**, S13.

Kel, A. E., Stegmaier, P., Valeev, T., Koschmann, J., Poroikov, V., Kel-Margoulis, O. V. and Wingender, E. (2016). Multi-omics "upstream analysis" of regulatory genomic regions helps identifying targets against methotrexate resistance of colon cancer. *EuPA Open Proteom* **13**, 1-13.

Koschmann, J., Bhar, A., Stegmaier, P., Kel, A. E. and Wingender, E. (2015). "Upstream Analysis": An Integrated Promoter-Pathway Analysis Approach to Causal Interpretation of Microarray Data. *Microarrays (Basel)* **4**, 270-86.

Krull, M., Pistor, S., Voss, N., Kel, A., Reuter, I., Kronenberg, D., Michael, H., Schwarzer, K., Potapov, A., Choi, C. et al. (2006). TRANSPATH: an information resource for storing and visualizing signaling pathways and their pathological aberrations. *Nucleic Acids Res* **34**, D546-51.

Lee, J. C., Biasci, D., Roberts, R., Gearry, R. B., Mansfield, J. C., Ahmad, T., Prescott, N. J., Satsangi, J., Wilson, D. C., Jostins, L. et al. (2017). Genome-wide association study identifies distinct genetic contributions to prognosis and susceptibility in Crohn's disease. *Nat Genet* **49**, 262-268.

Leiper, K., Martin, K., Ellis, A., Watson, A. J., Morris, A. I. and Rhodes, J. M. (2008). Clinical trial: randomized study of clarithromycin versus placebo in active Crohn's disease. *Aliment Pharmacol Ther* **27**, 1233-9.

Leiper, K., Morris, A. I. and Rhodes, J. M. (2000). Open label trial of oral clarithromycin in active Crohn's disease. *Aliment Pharmacol Ther* **14**, 801-6.

Lev Bar-Or, R., Maya, R., Segel, L. A., Alon, U., Levine, A. J. and Oren, M. (2000). Generation of oscillations by the p53-Mdm2 feedback loop: a theoretical and experimental study. *Proc Natl Acad Sci U S A* **97**, 11250-5.

Lin, X., Lu, J., Yang, M., Dong, B. R. and Wu, H. M. (2015). Macrolides for diffuse panbronchiolitis. *Cochrane Database Syst Rev* **1**, CD007716.

Long, M. D., Kappelman, M. D., Martin, C. F., Chen, W., Anton, K. and Sandler, R. S. (2016). Role of Nonsteroidal Anti-Inflammatory Drugs in Exacerbations of Inflammatory Bowel Disease. *J Clin Gastroenterol* **50**, 152-6.

Marteau, P., Probert, C. S., Lindgren, S., Gassul, M., Tan, T. G., Dignass, A., Befrits, R., Midhagen, G., Rademaker, J. and Foldager, M. (2005). Combined oral and enema treatment with Pentasa (mesalazine) is superior to oral therapy alone in patients with extensive mild/moderate active ulcerative colitis: a randomised, double blind, placebo controlled study. *Gut* **54**, 960-5.

McDaniel, D. K., Eden, K., Ringel, V. M. and Allen, I. C. (2016). Emerging Roles for Noncanonical NF-kappaB Signaling in the Modulation of Inflammatory Bowel Disease Pathobiology. *Inflamm Bowel Dis* **22**, 2265-79.

Mencarelli, A., Distrutti, E., Renga, B., Cipriani, S., Palladino, G., Booth, C., Tudor, G., Guse, J. H., Hahn, U., Burnet, M. et al. (2011). Development of non-antibiotic macrolide that corrects inflammation-driven immune dysfunction in models of inflammatory bowel diseases and arthritis. *Eur J Pharmacol* **665**, 29-39.

Merga, Y. J., O'Hara, A., Burkitt, M. D., Duckworth, C. A., Probert, C. S., Campbell, B. J. and Pritchard, D. M. (2016). Importance of the alternative NF-kappaB activation pathway in inflammation-associated gastrointestinal carcinogenesis. *Am J Physiol Gastrointest Liver Physiol* **310**, G1081-90.

Minshawi, F., White, M. R. H., Muller, W., Humphreys, N., Jackson, D., Campbell, B. J., Adamson, A. and Papoutsopoulou, S. (2019). Human TNF-Luc reporter mouse: A new model to quantify inflammatory responses. *Sci Rep* **9**, 193.

Nelson, D. E., Ihekwaba, A. E., Elliott, M., Johnson, J. R., Gibney, C. A., Foreman, B. E., Nelson, G., See, V., Horton, C. A., Spiller, D. G. et al. (2004). Oscillations in NF-kappaB signaling control the dynamics of gene expression. *Science* **306**, 704-8.

Oakley, G. M., Harvey, R. J. and Lund, V. J. (2017). The Role of Macrolides in Chronic Rhinosinusitis (CRSsNP and CRSwNP). *Curr Allergy Asthma Rep* **17**, 30.

Papoutsopoulou, S., Burkitt, M. D., Bergey, F., England, H., Hough, R., Schmidt, L., Spiller, D. G., White, M. H. R., Paszek, P., Jackson, D. A. et al. (2019). Macrophage-Specific NF-kappaB Activation Dynamics Can Segregate Inflammatory Bowel Disease Patients. *Front Immunol* **10**, 2168.

Peng, Y. C., Ho, S. P., Shyu, C. L., Chang, C. S. and Huang, L. R. (2014). Clarithromycin modulates Helicobacter pylori-induced activation of nuclear factor-kappaB through classical and alternative pathways in gastric epithelial cells. *Clin Exp Med* **14**, 53-9.

Perkins, N. D. (2012). The diverse and complex roles of NF-kappaB subunits in cancer. *Nat Rev Cancer* **12**, 121-32.

Poroikov, V., Akimov, D., Shabelnikova, E. and Filimonov, D. (2001). Top 200 medicines: can new actions be discovered through computer-aided prediction? *SAR QSAR Environ Res* **12**, 327-44.

Selby, W., Pavli, P., Crotty, B., Florin, T., Radford-Smith, G., Gibson, P., Mitchell, B., Connell, W., Read, R., Merrett, M. et al. (2007). Two-year combination antibiotic therapy with clarithromycin, rifabutin, and clofazimine for Crohn's disease. *Gastroenterology* **132**, 2313-9.

Son, H. J., Sohn, S. H., Kim, N., Lee, H. N., Lee, S. M., Nam, R. H., Park, J. H., Song, C. H., Shin, E., Na, H. Y. et al. (2019). Effect of Estradiol in an Azoxymethane/Dextran Sulfate Sodium-Treated Mouse Model of Colorectal Cancer: Implication for Sex Difference in Colorectal Cancer Development. *Cancer Res Treat* **51**, 632-648.

Stegmaier, P., Kel, A., Wingender, E. and Borlak, J. (2013). A discriminative approach for unsupervised clustering of DNA sequence motifs. *PLoS Comput Biol* **9**, e1002958.

Targan, S. R., Hanauer, S. B., van Deventer, S. J., Mayer, L., Present, D. H., Braakman, T., DeWoody, K. L., Schaible, T. F. and Rutgeerts, P. J. (1997). A short-term study of chimeric monoclonal antibody cA2 to tumor necrosis factor alpha for Crohn's disease. Crohn's Disease cA2 Study Group. *N Engl J Med* **337**, 1029-35.

Truelove, S. C. and Witts, L. J. (1955). Cortisone in ulcerative colitis; final report on a therapeutic trial. *Br Med J* **2**, 1041-8.

Turner, D., Walsh, C. M., Steinhart, A. H. and Griffiths, A. M. (2007). Response to corticosteroids in severe ulcerative colitis: a systematic review of the literature and a meta-regression. *Clin Gastroenterol Hepatol* **5**, 103-10.

van Deen, W. K., van Oijen, M. G., Myers, K. D., Centeno, A., Howard, W., Choi, J. M., Roth, B. E., McLaughlin, E. M., Hollander, D., Wong-Swanson, B. et al. (2014). A nationwide 2010-2012 analysis of U.S. health care utilization in inflammatory bowel diseases. *Inflamm Bowel Dis* **20**, 1747-53.

Williams, J. M., Duckworth, C. A., Vowell, K., Burkitt, M. D. and Pritchard, D. M. (2016). Intestinal Preparation Techniques for Histological Analysis in the Mouse. *Curr Protoc Mouse Biol* **6**, 148-168.

Williams, J. M., Duckworth, C. A., Watson, A. J., Frey, M. R., Miguel, J. C., Burkitt, M. D., Sutton, R., Hughes, K. R., Hall, L. J., Caamano, J. H. et al. (2013). A mouse model of pathological small intestinal epithelial cell apoptosis and shedding induced by systemic administration of lipopolysaccharide. *Dis Model Mech* **6**, 1388-99.

Figures

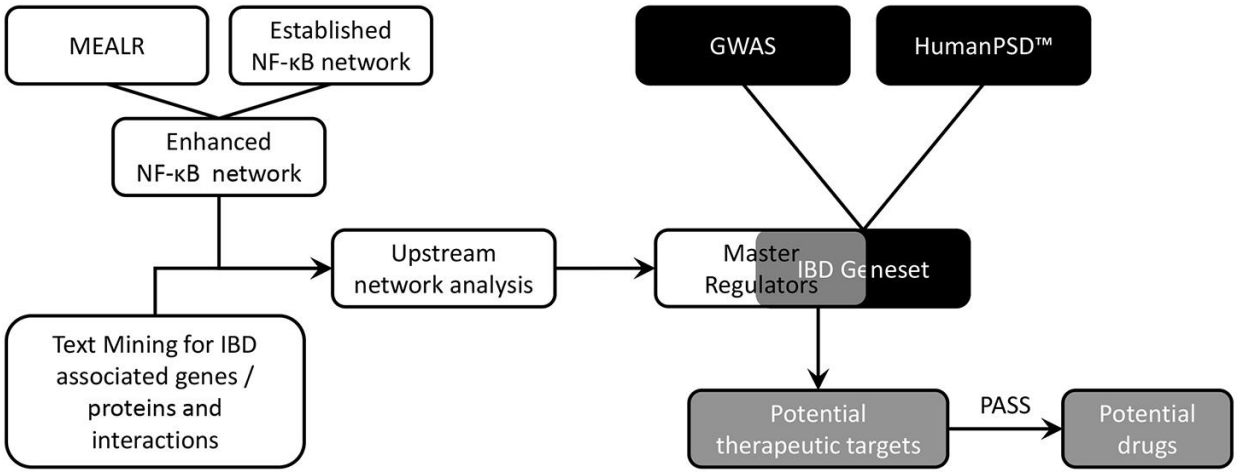

Figure 1: Schematic representation of the bioinformatic approach to identifying drugs with the potential to modulae IBD and NF-κB signalling.

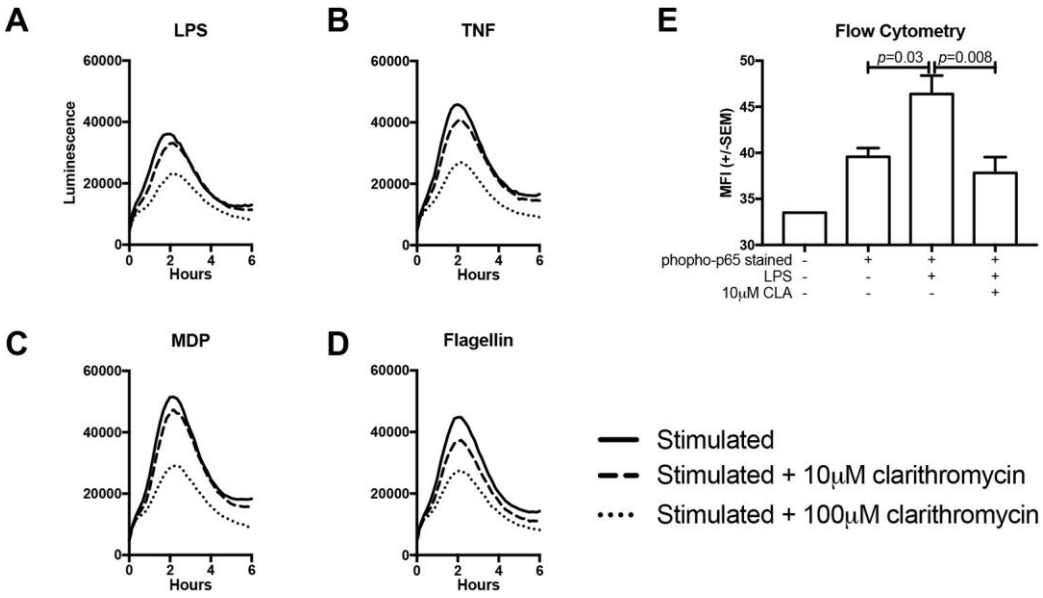

Figure 2. A-D: Luciferase activation curves for peritoneal macrophages extracted from HTNF.LucBAC mice stimulated with 10ng/mL LPS (**A**), 40 ng/mL TNF (**B**), 10µg/mL MDP (**C**) or 500ng/ml flagellin (**D**). Solid lines indicate cells response of pre-treated with drug vehicle (DMSO), dashed and dotted lines responses generated from cells pre-treated with 10µM or 100 µM clarithromycin, respectively. **E:** Median fluorescence intensity for anti-phopsho-p65 antibody stained peritoneal macrophages from C57BL/6 mice either unstimulated or stimulated with LPS and pre-treated with 10µM clarithromycin or DMSO vehicle. N=4 mice. Statistically significant differences tested by 1-way ANOVA and Dunnett's post hoc test.

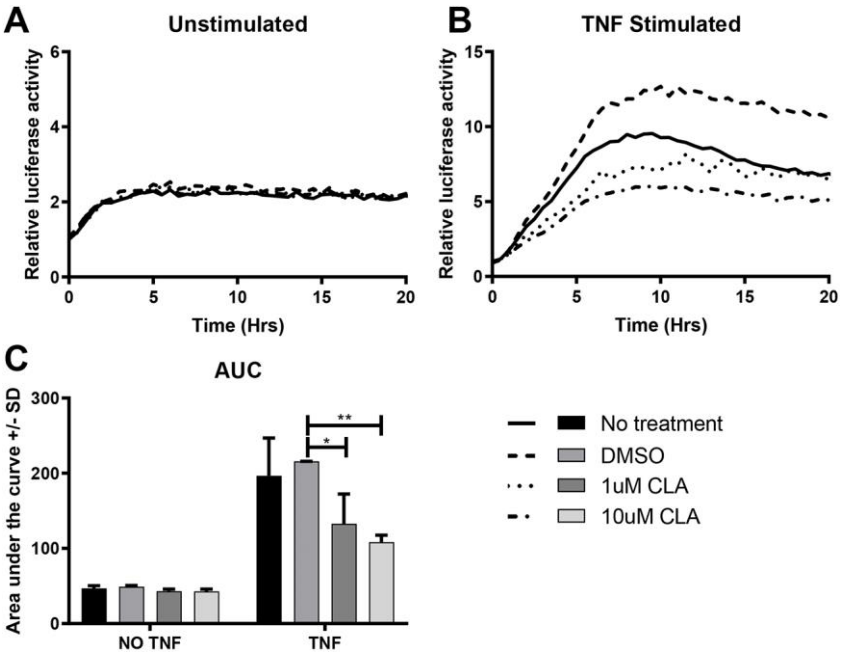

Figure 3: Representative luciferase activation curves for enteroids derived from HTNF.LucBAC mice either unstimulated (**A**) or stimulated with 100ng/mL TNF (**B**), and without pre-treatment (solid line) or 30 min pre-treatment with, DMSO vehicle (dashed line), 1µM clarithromycin (dotted line) or 10µM clarithromycin (dotted and dashed line). **C:** Area under the curve (AUC) calculations for the same experiment. N=3. Statistically significant differences tested by 2-way ANOVA and Dunnett's posthoc test.

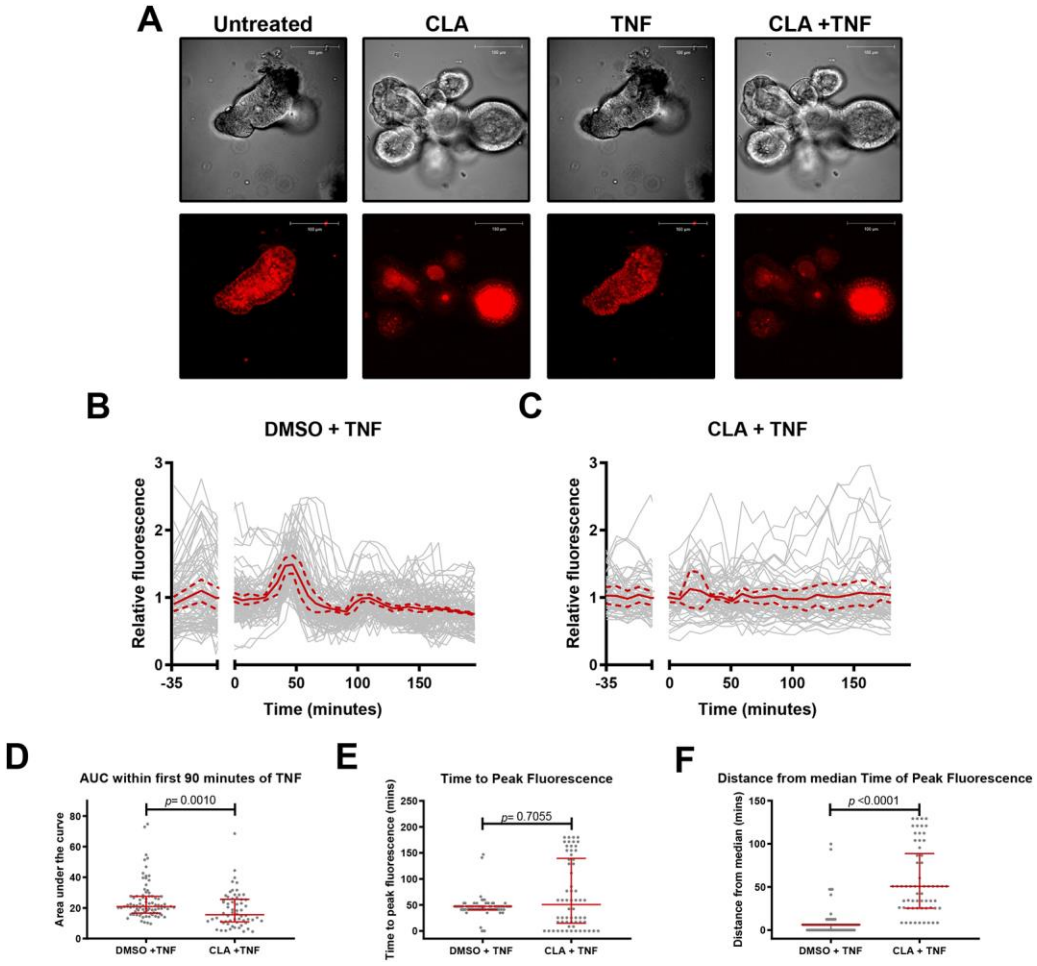

Figure 4 A: Representative images of bright field (upper panels) and red channel (lower panels) images of dynamic, live-cell imaging studies of enteroids derived from p65-DsRedxp/ IκBalpha-eGFP mice, either untreated, treated with clarithromycin alone, treated with 100ng/mL TNF alone, or pre-treated with 10µM clarithromycin and subsequently stimulated with TNF. **B and C:** Relative nuclear red fluorescence curves for individual cells (grey lines), mean (solid red line) and 1 SD above and below the mean (dashed red lines) over time. Cells pre-treated with DMSO vehicle **(B)** or clarithromycin **(C)** at time -35 min and stimulated with TNF at time 0 min. **D:** Area under the curve calculations for individual cells between time 0 and time 90 min for panels B and C. Statistically significant differences tested by Mann-Whitney U test. **E:** Time to peak fluorescence, post-TNF stimulation for individual cells, statistically significant differences tested by Mann-Whitney U test. **F:** Distance of individual

cells peak fluorescence from the median value, statistically significant differences tested by Mann-Whitney U test. N=88 vehicle pre-treated, 62 clarithromycin pre-treated cells for panels D-F, lines represent median and IQR for these panels.

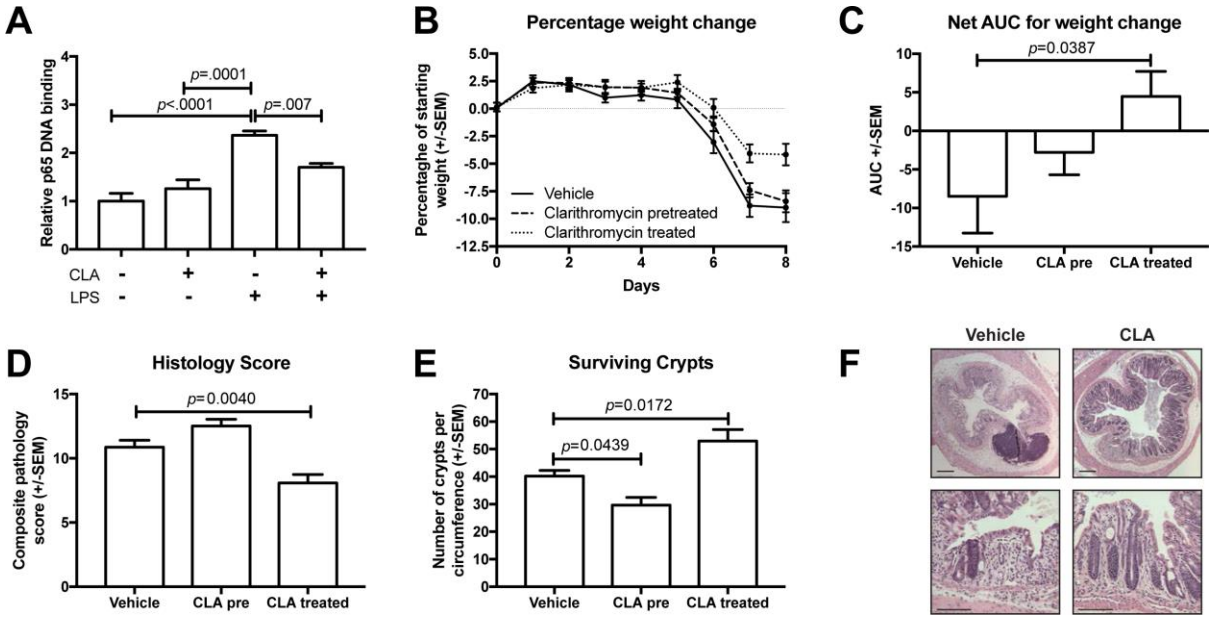

Figure 5A: Relative p65 DNA binding activity in whole-cell lysates from proximal small intestine of C57BL/6 mice pretreated for three days with 50mg/kg clarithromycin or saline vehicle, and subsequently injected i.p. with 0.125mg/kg LPS or vehicle. N=5-6. **B-F:** Effect of clarithromycin on outcomes of DSS colitis in C57BL/6 mice. **B:** Weight loss plotted over time. **C:** Area under the curve analysis of weight loss. **D:** Histology severity scores. **E:** Number of surviving crypts per colonic circumference. **F:** Representative photomicrographs of the colonic mucosa of DSS treated mice co-treated with saline vehicle or 10mg/kg clarithromycin by oro-gastric gavage. N=9-10. Statistically significant differences tested by 1-way ANOVA and Dunnett's post hoc test in all panels.

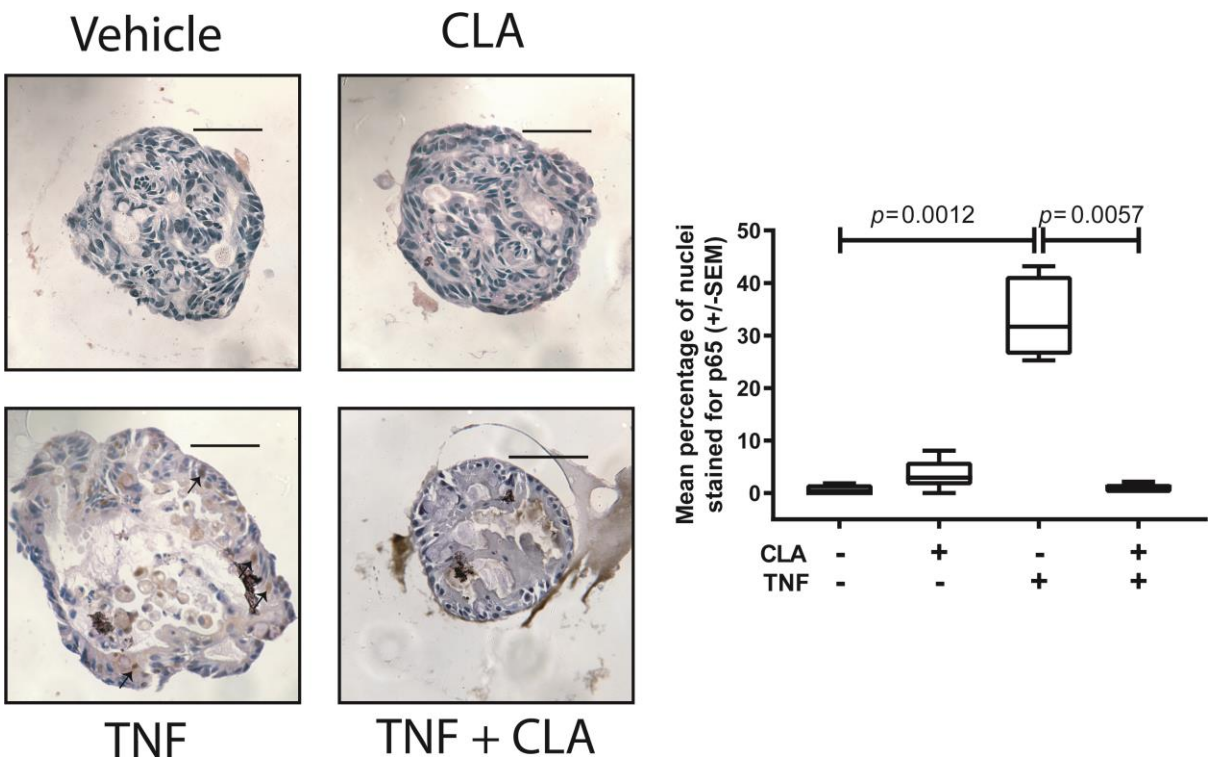

Figure 6A: Representative photomicrographs of human ileal enteroids either unstimulated or stimulated with 100ng/ml TNF, and either co-administered DMSO vehicle or 10µM clarithromycin and immunostained for total p65. **B:** Quantification of nuclear p65 staining of human enteroids. Statistical testing by Kruskal-Wallis 1-way ANOVA and Dunn's post hoc, N=6.

ID	Gene symbol
ENSG00000156273	*BACH1*
ENSG00000164330	*EBF1*
ENSG00000134954	*ETS1*
ENSG00000175592	*FOSL1*
ENSG00000154727	*GABPA*
ENSG00000104064	*GABPB1*
ENSG00000125347	*IRF1*
ENSG00000168310	*IRF2*
ENSG00000137265	*IRF4*
ENSG00000128604	*IRF5*
ENSG00000185507	*IRF7*
ENSG00000140968	*IRF8*
ENSG00000213928	*IRF9*
ENSG00000177606	*JUN*
ENSG00000171223	*JUNB*
ENSG00000130522	*JUND*
ENSG00000109320	*NFKB1*
ENSG00000077150	*NFKB2*
ENSG00000162924	*REL*
ENSG00000173039	*RELA*
ENSG00000104856	*RELB*
ENSG00000159216	*RUNX1*
ENSG00000020633	*RUNX3*
ENSG00000269404	*SPIB*

Table 1: Transcription factors predicted to contribute to NF-κB regulatory cascades by MEALR analysis

ID	Gene symbol	# consensus NF-κB/RelA sites within 10kb from gene
ENSG00000005339	*CREBBP*	1
ENSG00000015475	*BID*	2
ENSG00000030110	*BAK1*	1
ENSG00000034152	*MAP2K3*	1
ENSG00000049759	*NEDD4L*	3
ENSG00000051382	*PIK3CB*	1
ENSG00000051523	*CYBA*	1
ENSG00000069399	*BCL3*	2
ENSG00000077150	*NFKB2*	2
ENSG00000081059	*TCF7*	3
ENSG00000082701	*GSK3B*	1
ENSG00000083799	*CYLD*	1
ENSG00000084676	*NCOA1*	2
ENSG00000099341	*PSMD8*	1
ENSG00000100324	*TAB1*	2
ENSG00000100365	*NCF4*	2
ENSG00000100387	*RBX1*	1
ENSG00000101849	*TBL1X*	1
ENSG00000102871	*TRADD*	1
ENSG00000104365	*IKBKB*	2
ENSG00000104825	*NFKBIB*	1
ENSG00000104856	*RELB*	2
ENSG00000105647	*PIK3R2*	1
ENSG00000107263	*RAPGEF1*	3
ENSG00000109320	*NFKB1*	2
ENSG00000109332	*UBE2D3*	2
ENSG00000110330	*BIRC2*	1
ENSG00000111186	*WNT5B*	1
ENSG00000112062	*MAPK14*	1
ENSG00000115415	*STAT1*	2
ENSG00000116473	*RAP1A*	2
ENSG00000116701	*NCF2*	1
ENSG00000118260	*CREB1*	1
ENSG00000118503	*TNFAIP3*	2
ENSG00000119487	*MAPKAP1*	3
ENSG00000121879	*PIK3CA*	1
ENSG00000124486	*USP9X*	1
ENSG00000125084	*WNT1*	1
ENSG00000125347	*IRF1*	1
ENSG00000127191	*TRAF2*	2
ENSG00000127666	*TICAM1*	1

ENSG00000131323	*TRAF3*	5
ENSG00000131508	*UBE2D2*	1
ENSG00000134070	*IRAK2*	2
ENSG00000136689	*IL1RN*	1
ENSG00000136807	*CDK9*	1
ENSG00000136810	*TXN*	1
ENSG00000137275	*RIPK1*	2
ENSG00000141510	*TP53*	1
ENSG00000142453	*CARM1*	1
ENSG00000144802	*NFKBIZ*	2
ENSG00000145675	*PIK3R1*	1
ENSG00000146232	*NFKBIE*	1
ENSG00000148053	*NTRK2*	1
ENSG00000148737	*TCF7L2*	1
ENSG00000150991	*UBC*	1
ENSG00000154589	*LY96*	1
ENSG00000157764	*BRAF*	1
ENSG00000161011	*SQSTM1*	1
ENSG00000162736	*NCSTN*	1
ENSG00000162924	*REL*	2
ENSG00000163932	*PRKCD*	3
ENSG00000164327	*RICTOR*	1
ENSG00000166167	*BTRC*	1
ENSG00000168036	*CTNNB1*	1
ENSG00000169967	*MAP3K2*	1
ENSG00000170315	*UBB*	1
ENSG00000171552	*BCL2L1*	2
ENSG00000171608	*PIK3CD*	2
ENSG00000172936	*MYD88*	1
ENSG00000173039	*RELA*	1
ENSG00000174130	*TLR6*	1
ENSG00000177606	*JUN*	1
ENSG00000183207	*RUVBL2*	1
ENSG00000185338	*SOCS1*	1
ENSG00000185507	*IRF7*	1
ENSG00000185627	*PSMD13*	1
ENSG00000186197	*EDARADD*	1
ENSG00000196470	*SIAH1*	1
ENSG00000197153	*HIST1H3J*	2
ENSG00000197409	*HIST1H3D*	3
ENSG00000197442	*MAP3K5*	3
ENSG00000198400	*NTRK1*	1
ENSG00000205155	*PSENEN*	2
ENSG00000213281	*NRAS*	1
ENSG00000226979	*LTA*	4
ENSG00000227507	*LTB*	3

ENSG00000232810	*TNF*	4
ENSG00000243414	*TICAM2*	2
ENSG00000263528	*IKBKE*	3

Table 2: NF-κB target genes identified by MEALR to be involved in regulatory cascades

Ranking	Drug
1	Clarithromycin
2	Budesonide
3	Digoxin
4	Dexamethasone
5	Triamcinolone acetonide
6	Methylprednisolone
7	Prednisone
8	Azithromycin
9	Medroxyprogesterone
10	Estradiol
11	Nystatin
12	Progesterone
13	Albuterol
14	Ibuprofen
15	Dicyclomine
16	Naproxen
17	Nabumetone
18	Propranolol
19	Metoprolol
20	Atenolol
21	Acetaminophen
22	Phentermine
23	Divalproex
24	Gabapentin
25	Diclofenac
26	Lisdexamfetamine
27	Pregabalin
28	Methocarbamol
29	Metformin

Table 3: Drugs predicted to influence IBD.

Supplementary figures

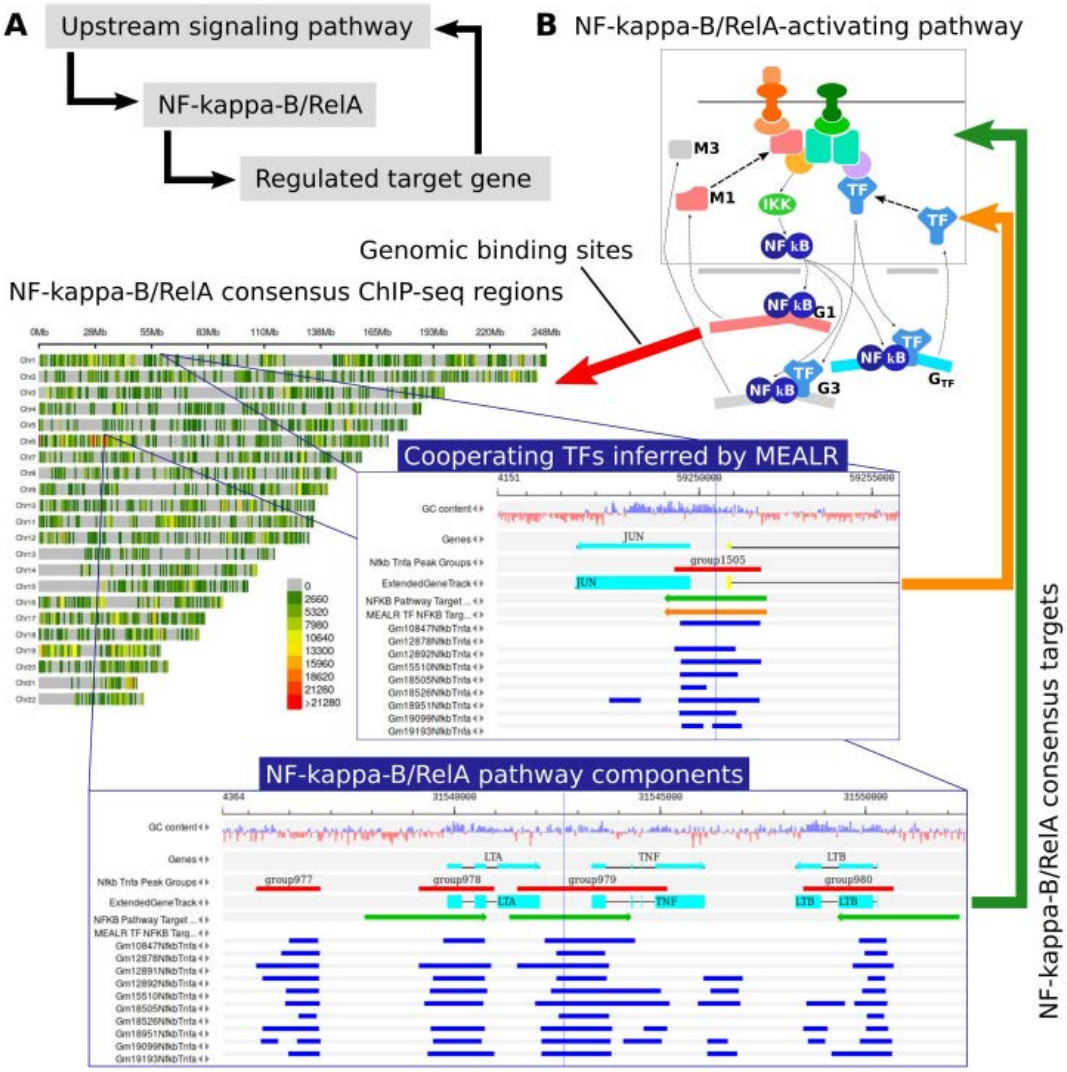

Figure S1: Schematic of the transcriptional feedback loops sought by our analysis. Upon activation through upstream signalling cascades the transcriptional regulator NF-kappa-B/RelA (and cooperating transcription factors) control expression of target genes which may themselves play a role in signalling cascades regulating the activity of NF-kappa-B/RelA thereby establishing a positive or negative feedback loop depending on whether NF-kappa-B/RelA enhances or interferes with the transcription of respective target genes. **B:** More detailed illustration of identified feedback loops. Using consensus NF-kappa-B/RelA binding sites collected from 10 ChIP-seq experiments we analysed their genomic locations with respect to nearby potential target genes which were known components of relevant pathways and/or transcription factors whose motifs played a role for target sequence recognition as inferred by MEALR. Details of the compiled and analysed data are exemplified for pathway target genes TNF, LTA and LTB on chromosome 6 and for the cooperating transcription factor JUN on chromosome 1. The consensus peak density presentation was calculated using the CMplot package. The detailed views of genomic regions were created using the genome browser of the geneXplain platform.

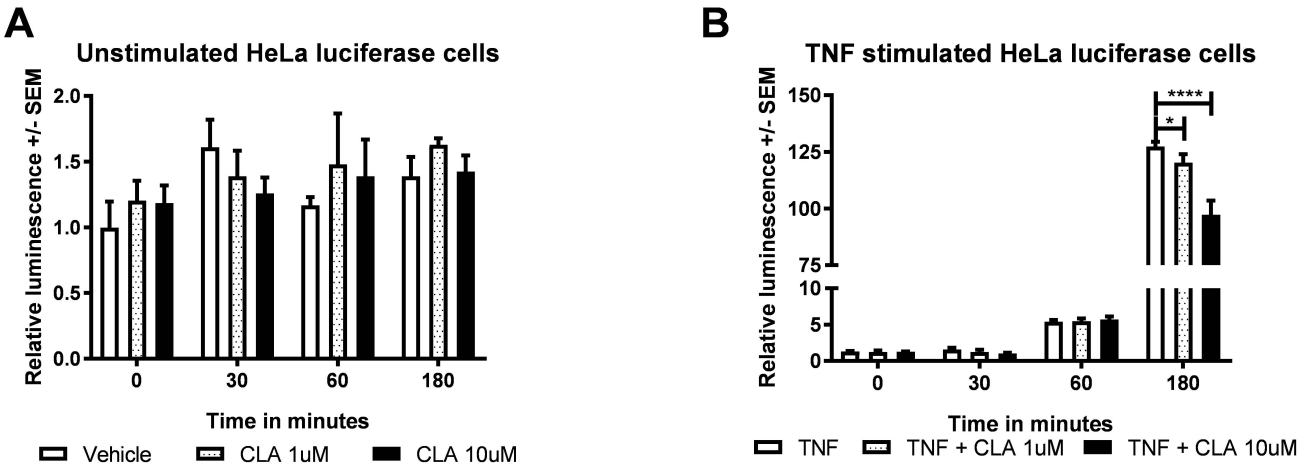

Figure S2: Relative luciferase activity in unstimulated HeLa cells treated with DMSO vehicle (open bar), 1uM (hatched bar) or 10uM (solid bar) clarithromycin. B: Relative luciferase activity in TNF stimulated HeLa cells treated with DMSO vehicle, 1uM or 10uM CLA. * denotes p<.05, ****p<.0001, by 2-way ANOVA and Dunnett's posthoc test.

Movie 1: Representative timelapse confocal video of red channel images of dynamic, live-cell imaging studies of enteroids derived from p65-DsRedxp/ IκBalpha-eGFP mice, either treated with 100ng/mL TNF alone, or pre-treated with 10µM clarithromycin and subsequently stimulated with TNF.

Table S1: NF-κB co-operating transcription factors identified by MEALR

Click here to Download Table S1

Table S2: Interactions between genes and or proteins identified by text mining algorithm

Click here to Download Table S2

Table S3: Controlling node genes that may regulate signalling activity on the NF-κB network

Click here to Download Table S3

Table S4: IBD target genes, with source of data

Click here to Download Table S4

Table S5: List of IBD key-nodes, potential therapeutic targets for IBD

Click here to Download Table S5

Table S6: IBD key-nodes and their associated PASS activities

Click here to Download Table S6